Electronic Supplementary Material (ESI) for Dalton Transactions.

Supporting Information

for

N-Atom Transfer via Thermal or Photolytic Activation of a Co-Azido Complex with a PNP Pincer Ligand

Vincent Vreeken, [a] Lambert Baij,[a], Bas de Bruin,[a] Maxime A. Siegler,[a] Jarl Ivar van der Vlugt*,[a]

1. General methods

With exception of the compounds given below, all reagents were purchased from commercial suppliers and used without further purification. All experiments were conducted under inert atmosphere, either by using Schlenk techniques or by using a Glovebox under N_2 pressure. **PN^HP^{iPr}** (bis(2-di*iso*propylphosphino-4-methylphenyl)amine)[S1] was synthesized according to literature procedures. Toluene, tetrahydrofuran, diethylether and pentane were distilled from sodium benzophenone ketyl. CH_2Cl_2 was distilled from CaH_2. NMR spectra (^1H, $^1H\{^{31}P\}$, $^{13}C\{^1H\}$, $^{31}P\{^1H\}$)) were measured on a Bruker DRX 500, Bruker AV 400, Bruker DRX 300 or on a Bruker AV 300 spectrometer at room temperature, unless noted otherwise. Experimental X-band EPR spectra were recorded on a Bruker EMX spectrometer equipped with a cryostat (Oxford Instruments). The EPR spectra were simulated by iteration of the anisotropic g-values, (super)hyperfine coupling constants, and line widths using the EPR simulation program W95EPR developed by the group of Prof.Dr. F. Neese. High resolution mass spectra were recorded on a JEOL AccuTOF LC, JMS-T100LP Mass spectrometer using cold spray ionization (CSI) and electron spray ionization (ESI) and on a JEOL AccuTOF GC v 4g, JMS-T100GCV Mass spectrometer using field desorption (FD). IR spectra were either recorded with a Thermo Nicolet Nexus FT-IR spectrometer or with a Bruker Vertex 70. UV/visible spectra were recorded on a Hitachi U-3300 spectrophotometer. Cyclic voltammetry measurements were performed in THF containing $N(n\text{-}Bu)_4PF_6$ (0.1 M) at room temperature under a nitrogen atmosphere using a platinum disk working electrode, a platinum coil counter electrode and a silver coil reference electrode. All redox potentials are referenced to Fc/Fc^+. For the irradiation experiments a 500 W Hg/Xe lamp (Hamamatsu Photonics L8288) was used.

2. Synthesis and characterization of new compounds

*Synthesis of complex **1***

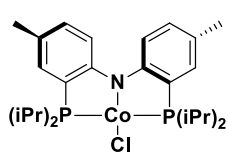

The synthesis was performed according to a modified literature procedure.[S2] A solution of **PN^{H}P^{iPr}** (1.66 g, 3.89 mmol) in THF (20 mL) was prepared and cooled to -78°C. Subsequently, n-BuLi (1.71 mL of a 2.5 M solution in hexanes, 4.28 mmol) was added to the solution. Then, a suspension of anhydrous $CoCl_2$ (0.505 g, 3.89 mmol) in THF (50 mL) was added via cannula and the reaction mixture was allowed to stir for 22h. The solvent was removed *in vacuo* and the product was extracted with toluene (50 mL). After filtration over Celite, the filtrate was concentrated to approx. 5 mL and stored overnight at -20 °C, yielding complex **1** as a dark-blue crystalline solid (1.63 g, 80%). The product was identified by comparing the ^{1}H NMR spectrum with the reported literature values.[S2]

*Synthesis of complex **2***

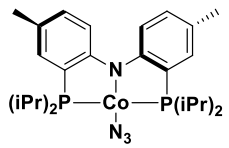

A Schlenk flask was charged with **1** (500 mg, 0.96 mmol) and NaN_3 (624 mg, 9.6 mmol). THF (20 mL) was added and the resulting suspension was stirred for 22h during which the color of the mixture changed from dark blue to dark green. Then, volatiles were removed *in vacuo*. The azido product was extracted with toluene and filtered over Celite. The filtrate was concentrated to approx. 5 mL and stored at -20 °C overnight, yielding a dark green solid 485 mg, 95%). The ^{15}N enriched azido complex **2-^{15}N** was prepared according to the same method by using ^{15}N-enriched sodium azide.

^{1}H NMR (400 MHz, C_6D_6, ppm): δ 29.6 ($\Delta_{½}$ = 270 Hz), 25.8 ($\Delta_{½}$ = 250 Hz), 12.3 ($\Delta_{½}$ = 50 Hz), 4.8 (bs), 3.3 (bs), -24.8 ($\Delta_{½}$ = 447 Hz); μ_{eff} = 1.77 μ_B (Evans' method, 24°C, C_6D_6); **EPR** g_{11} 3.000, g_{22} 2.008, g_{33} 1.950; $A^{Co}{}_1$ = 270 MHz, $A^{Co}{}_2$ = NR, $A^{Co}{}_3$ = NR (toluene, 20K); **HR-MS** (CSI) calcd for $[M]^+$ $C_{26}H_{40}CoN_4P_2$ *m/z*: 529.2060, found 529.2032; **FTIR** (N_3 stretch): (THF) *v* = 2052, 2025 (shoulder) cm^{-1} (Figure S3);[S3] (benzene) *v* = 2052 (broad) cm^{-1}, for **2-^{15}N** (THF): *v* = 2044, 2037 (shoulder) cm^{-1}.

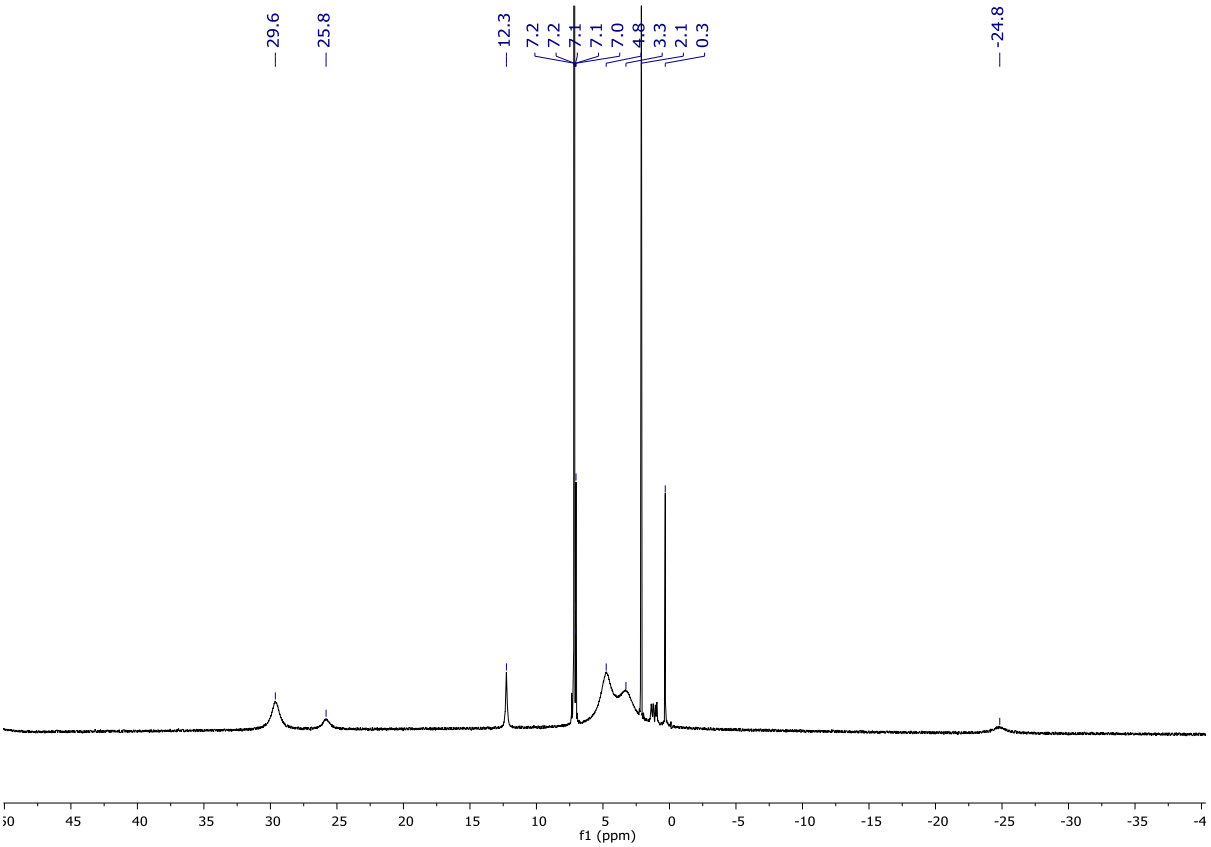

Figure S1. ^{1}H NMR spectrum of **2** (C_6D_6, 400 MHz, 298K). Residual peaks from toluene (7.1-7.0 ppm and 2.1 ppm) and grease (0.3 ppm) present.

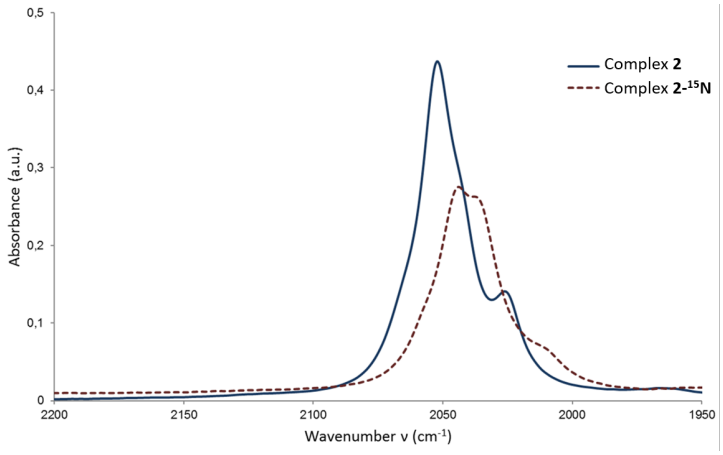

Figure S2. Solution IR spectrum of **2** (solid line) and **2-^{15}N** (dashed line) recorded in THF.

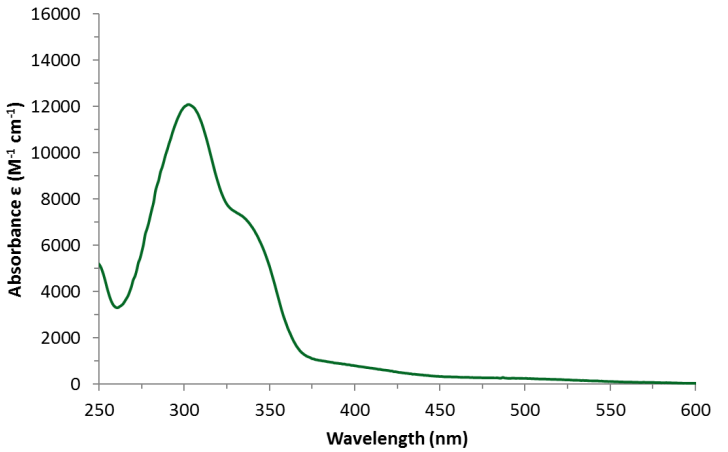

Figure S3. UV-vis spectrum of **2** in THF.

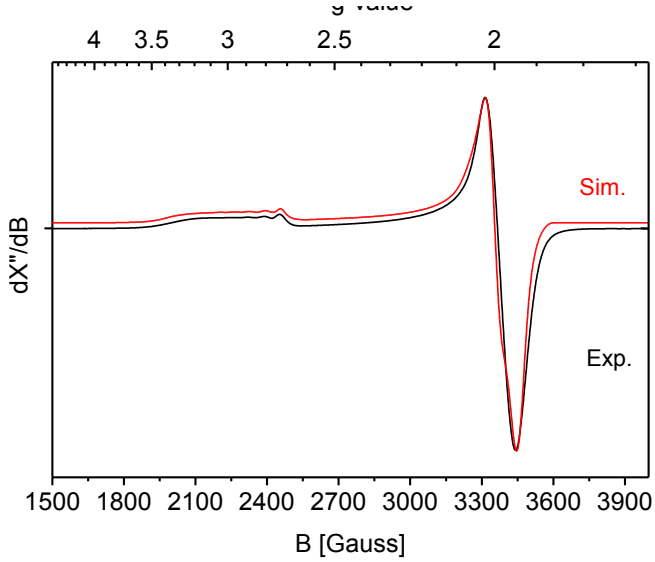

Figure S4. EPR spectrum of **2** in toluene at 20 K. Experimental parameters: Frequency = 9.386576 GHz, T = 20 K, Modulation Amplitude = 4.0 G, power = 0.6 mW. Simulated *g* values, hyperfine couplings A and linewidth parameters: g_{11} 3.000, g_{22} 2.008, g_{33} 1.950; $A^{Co}{}_1$ = 270 MHz, $A^{Co}{}_2$ = NR, $A^{Co}{}_3$ = NR; W_{11} = 55.00 G; W_{22} = 33.00 G; W_{33} = 33.00 G.

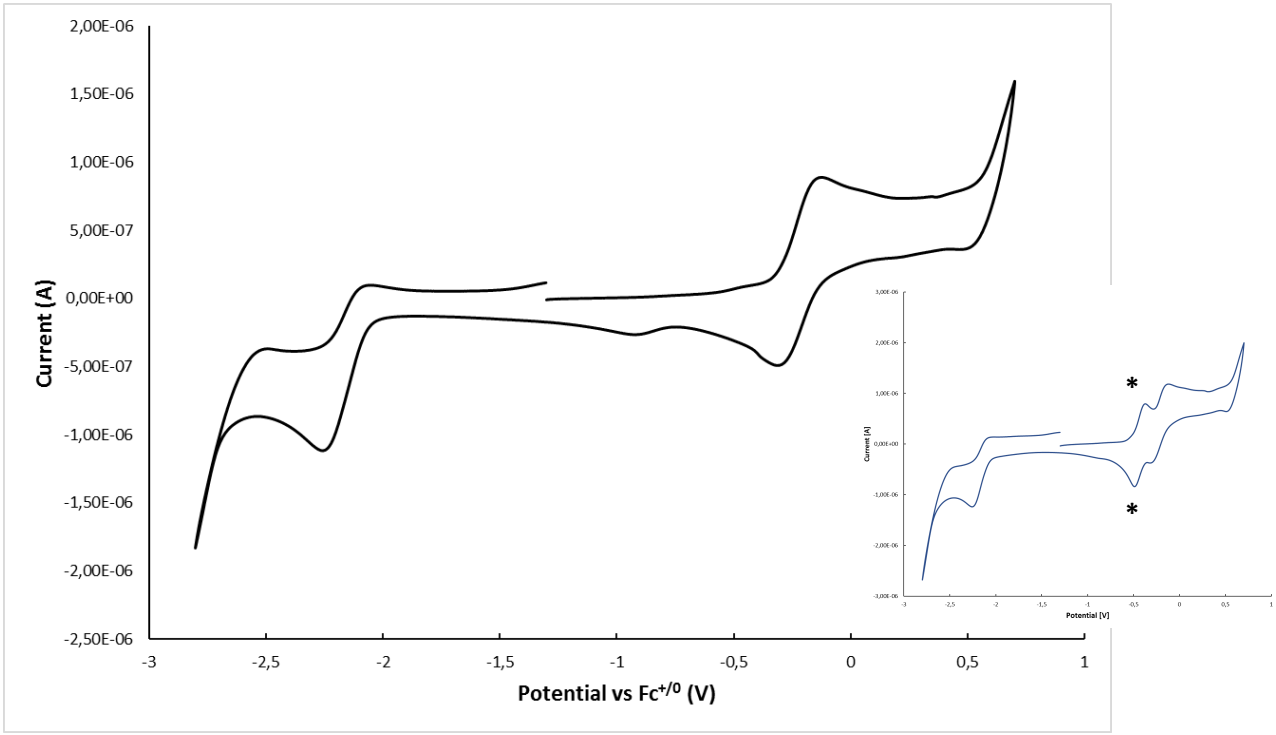

Figure S5. Cyclic voltammogram of **2** recorded in THF at 0.1 V/s on a platinum electrode and with NBu_4PF_6 as electrolyte. As internal standard decamethylferrocene ($Fc(Cp^*)_2$ was used (see insert) instead of the more usual ferrocene (Fc) to avoid overlapping waves of **2** with the internal standard.

*Synthesis of complex **3***

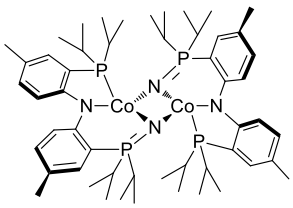

Thermolysis: A *J-Young* type Schlenk was loaded with complex **2** (150 mg, 0.28 mmol). The solid was heated to 180 °C. Around 110 °C the green solid melted and around 150 °C bubble formation was visible. At this point, the color changed from green to red. The temperature was maintained at 180 °C for 1 hour. Subsequently, the product was allowed to cool down and then extracted with pentane. Evaporation of the solvent yielded a dark red solid (124 mg, 88%). Crystals suitable for X-ray diffraction studies were grown from a pentane solution at -20 °C.

Photolysis: A *J-Young* type Schlenk-cuvette was charged with a dark green solution of complex **2** (11 mg, 0.02 mmol) in THF (2 mL). While stirring, the mixture was irradiated for 1.5 hours. During this period the color changed to dark red. The solvents was removed *in vacuo* and the resulting red solid was analyzed with ^{1}H NMR confirming the presence of complex **3** as the major product.

^{1}H NMR (400 MHz, C_6D_6, ppm): δ 24.61 (s, 1H), 12.26 (s, 1H), 10.02 (d, *J* = 7.5 Hz, 1H), 9.47 (s, 1H), 9.45 (s, 1H), 8.65 (s, 1H), 8.47 (d, *J* = 6.6 Hz, 1H), 7.14 (s, 1H), 5.72 (s, 3H), 4.73 (s, 1H), 4.43 (s, 3H), 4.37 (s, 3H), 3.81 (s, 3H), 3.52 (d, *J* = 8.1 Hz, 1H), 3.30 (s, 3H), 3.15 (s, 3H), 0.30 (s, 3H), -1.84 (s, 3H), -2.69 (s, 3H), -5.26 (s, 3H); μ_{eff} = 2.75

μ_B (Evans' method, 20°C, toluene); **HR-MS** (CSI) calcd for $[M + H]^+$ $C_{52}H_{81}Co_2N_4P_4$ *m/z*: 1003.4076, found 1003.5360.

The sensitivity of complex **3** interfered with attempts to analyze this species using CSI HR-MS. A very weak signal was found for the expected mass of **3** but the main species in the mass spectrum are free, oxidized ligand ($[^{O}PN^{H}PN^{H} + H]^+$ calculated *m/z*: 461.2851, found 461.2917) and cobalt complexes with this phosphinoxide ligand. Depending on the flow and addition of acetonitrile other species became more prominent. The mass spectrum of the thermolysis product of **2-^{15}N** confirmed the incorporation of azide-N into the ligand, as the $^{O}PN^{H}PN^{H}$ fragment shifts with one atomic mass unit to *m/z* 462.2613. This provides evidence for the azide being the source of the new P=N moiety.

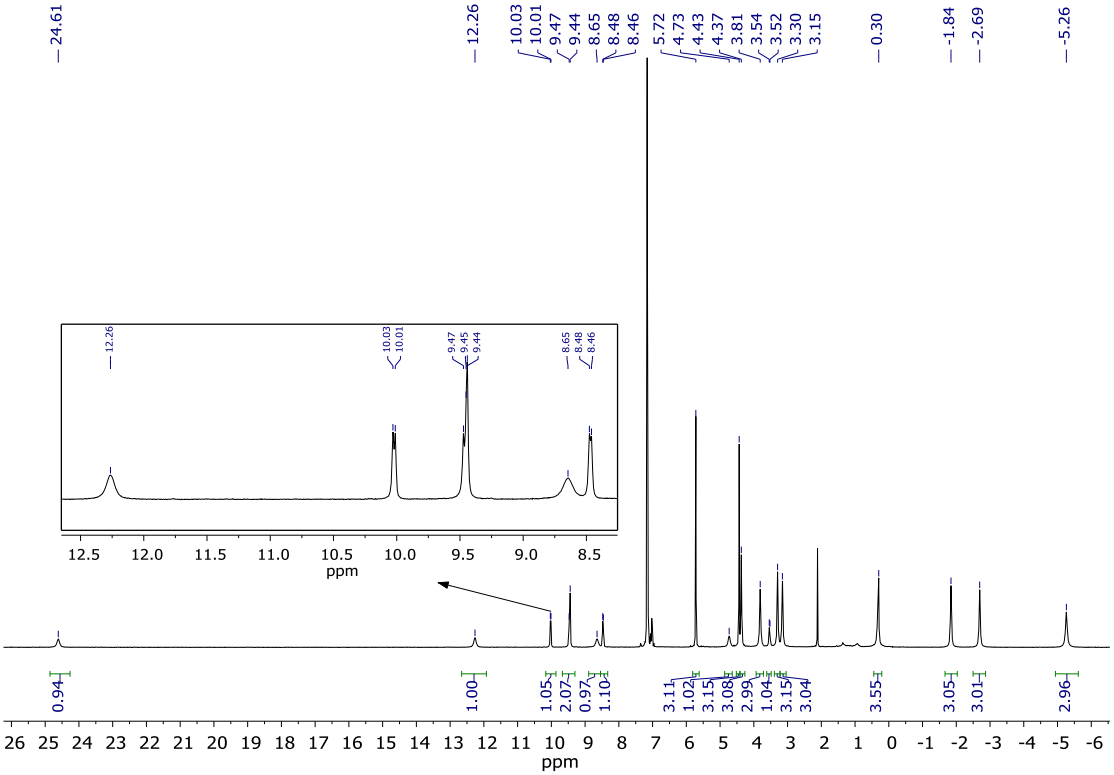

Figure S6. ^{1}H NMR spectrum of **3** (C_6D_6, 400 MHz, 298 K) (peaks of residual toluene present)

*Synthesis of complex **4***

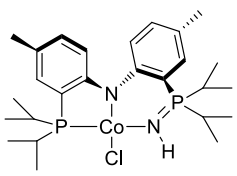

In a *J-Young* Schlenk complex **3** (53 mg, 0.053 mmol) was dissolved in Et_2O (2mL). To the red solution 2M HCl in Et_2O (53 µL, 0.106 mmol) was added, causing the formation of a light blue solid. The liquid phase remained dark red and was stirred for 1 hour. Then, the mixture was filtered and the solvent was evaporated. The crude solid was triturated with pentane and dried *in vacuo*, yielding **4** as a brown solid (32 mg, 56%). Red crystals suitable for X-ray analysis were obtained from a saturated Et_2O solution.

^{1}H NMR (400 MHz, C_6D_6, ppm): δ 43.85 ($\Delta_{½}$ = 24 Hz), 42.54 ($\Delta_{½}$ = 21 Hz), 34.73 ($\Delta_{½}$ = 25 Hz), 33.76 ($\Delta_{½}$ = 16 Hz), 24.62 ($\Delta_{½}$ = 40 Hz), 19.61 ($\Delta_{½}$ = 37 Hz), 3.25 ($\Delta_{½}$ = 55 Hz), -42.18 ($\Delta_{½}$ = 74 Hz); μ_{eff} = 4.28 μ_B (Evans' method, 24°C, C_6D_6); **HR-MS** (ESI) calcd for $[M]^+$ $C_{26}H_{41}Cl_1Co_1N_2P_2$ *m/z*: 537.17655, found 537.17288. **FTIR** (DCM): ν_{NH} 3375 cm^{-1}.

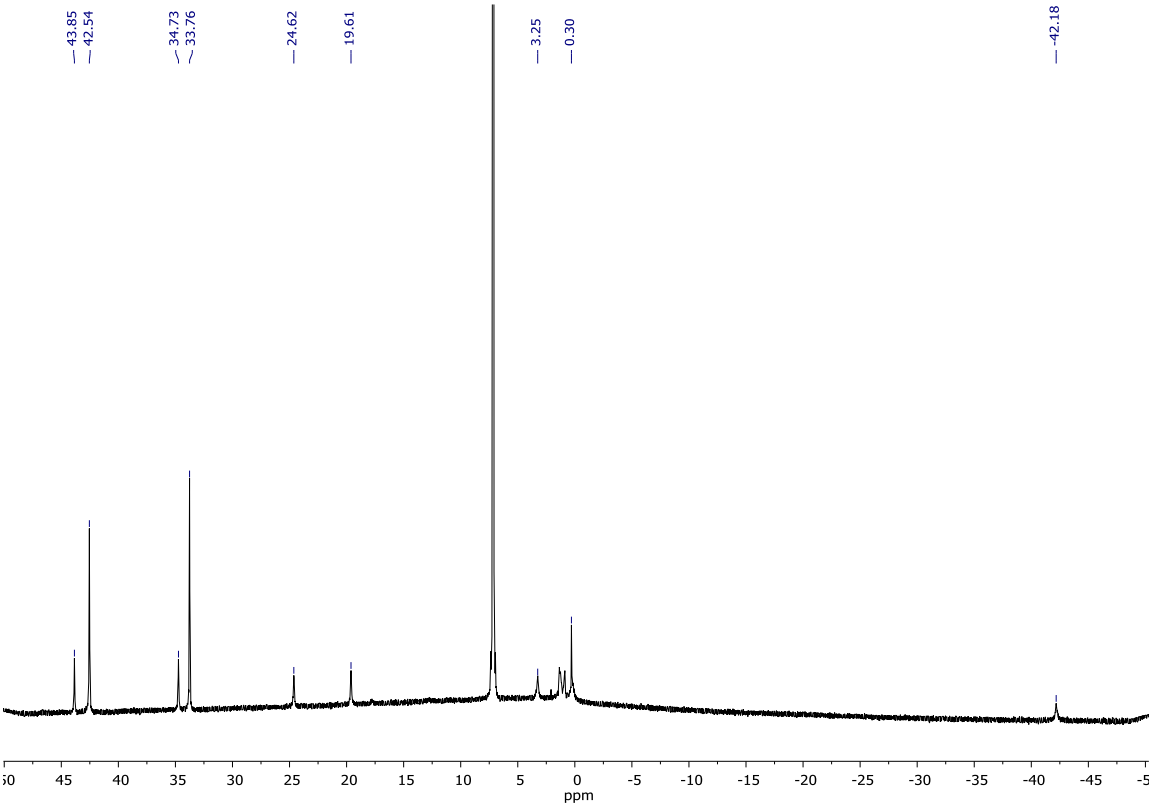

Figure S7. ^{1}H NMR spectrum of **4** (C_6D_6, 400 MHz, 298K)

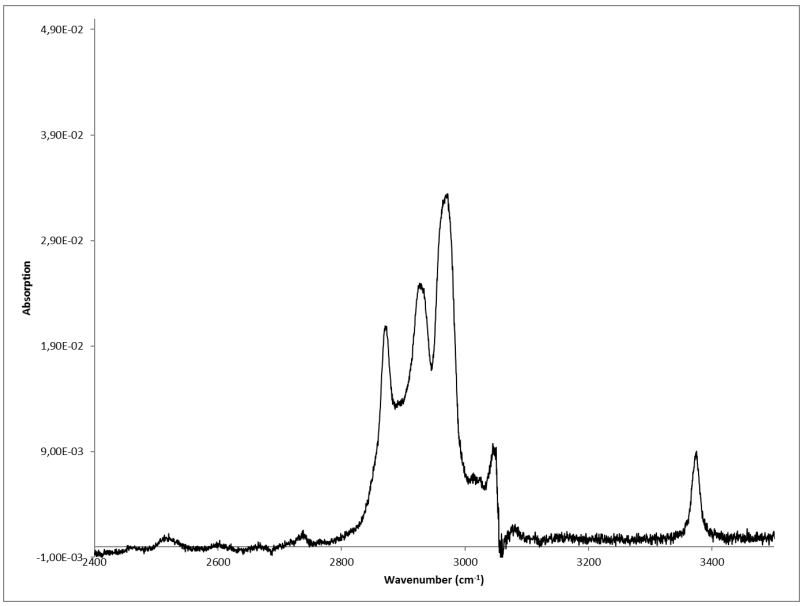

Figure S8. Solution IR spectrum of **4** in THF

3. Thermal Gravimetric Analysis-Differential Scanning Calorimetry measurements

The behavior of complex **2** at increased temperatures was monitored using Thermal Gravimetric Analysis (TGA) and Differential Scanning Calorimetry (DSC). The combination of these techniques is especially suited for reactions involving thermal decomposition of azides, as this is an exothermic event involving significant mass loss. The results of the TGA-DSC measurement of **2** are displayed in Figure S9. Examination of the scan reveals an endothermic event from 100 °C – 112 °C. This event can point at melting of the complex, although the loss of mass suggests that evaporation of water traces and of solvent residues (toluene, THF) may also take place. Subsequently, a clear exothermic event takes place starting at 169 °C. This event is associated with a mass change of -3.1 %, which is less than expected for pure N_2 release (-5.3 %). Despite this discrepancy, the combination of mass loss and energy release gives a valuable indication that decomposition of the N_3 group might take place around this temperature. The difference between the expected and the found mass-loss can probably be explained by a combination of the extreme sensitivity of **2**, affecting the purity of the compound measured (and hence the available azide), and a decreased accuracy of the machine at smaller quantities (<10 mg). Events at even higher temperatures likely involve other decomposition pathways of the complex.

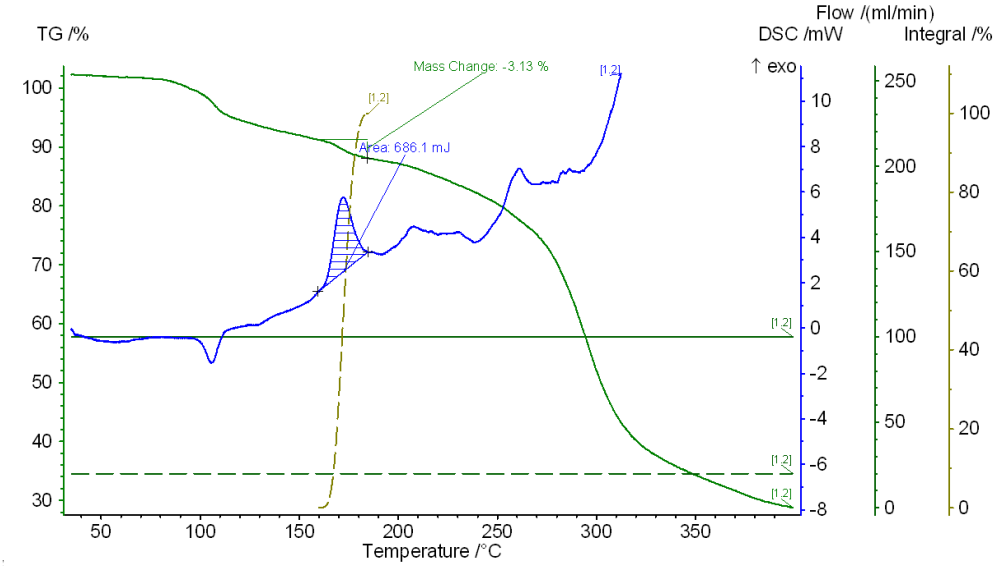

Figure S9. TGA-DSC measurement of **2** using 3K/min scan speed.

4. Variable temperature NMR measurements with complex 3

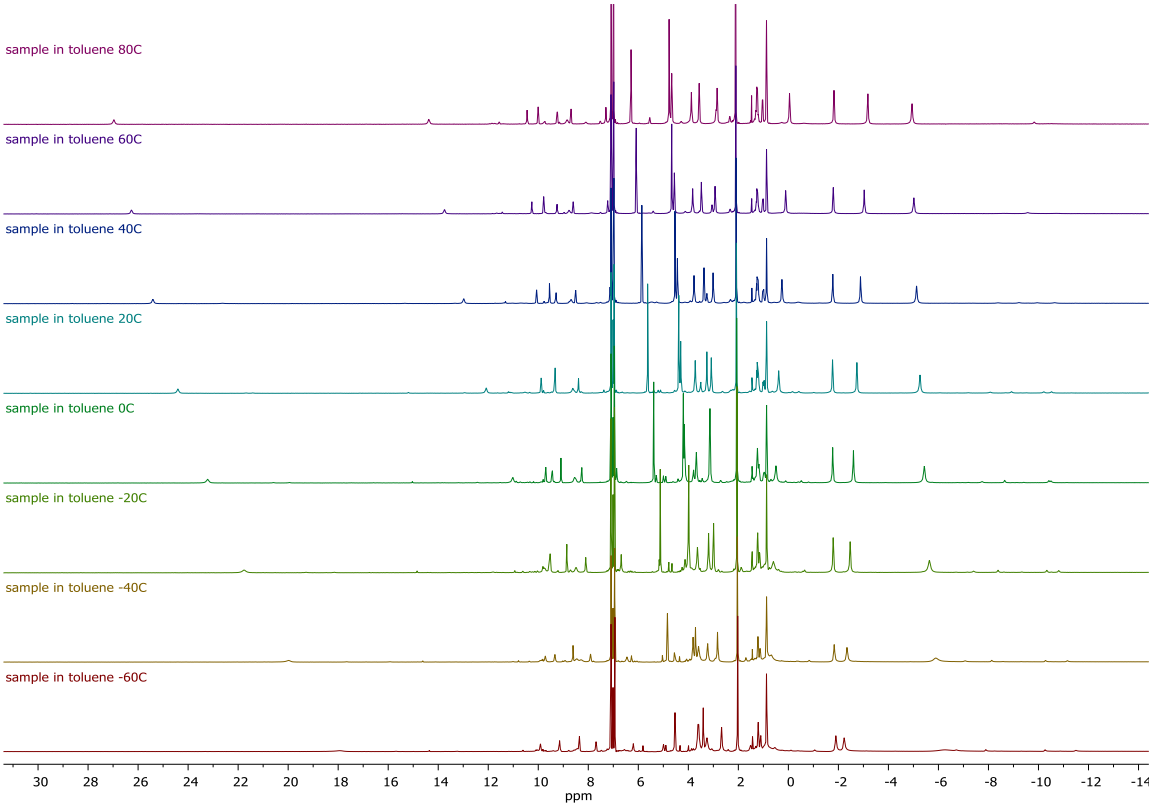

Figure S10. VT NMR spectra of **3** in toluene-d_8 ranging from -60 °C to 80 °C in steps of 20 °C

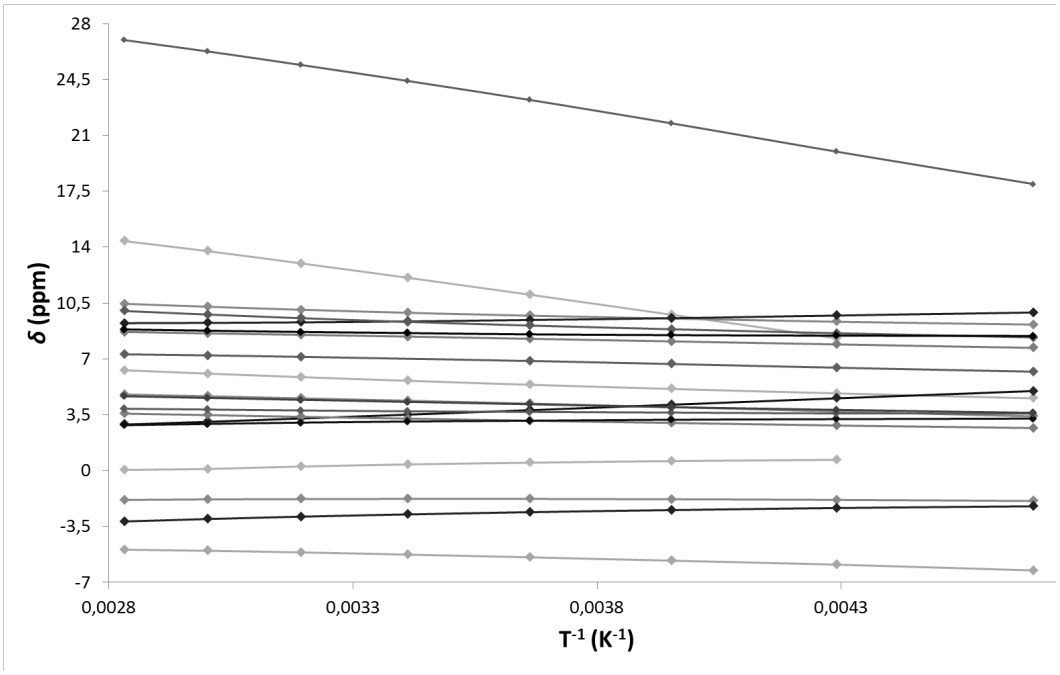

Figure S11. Temperature dependence of the ^{1}H NMR chemical shifts of complex **3** in toluene-d_8.

5. Computational details

Geometry optimizations were carried out with the Turbomole program package[S4] coupled to the PQS Baker optimizer[S5] via the BOpt package[S6] at the BP86[S7,S8] level. We used the def2-TZVP basis set.[S9,S10] Dispersion corrections were applied.[S11] All minima (no imaginary frequencies) and transition states (one imaginary frequency) were characterized by calculating the Hessian matrix. ZPE and gas-phase thermal corrections (entropy and enthalpy, 298 K, 1 bar) from these analyses were calculated. The nature of the transition states was confirmed by IRC calculations. The optimized geometries of all species are supplied as separate files in .pdb and .xyz format.

Mechanistic considerations

The starting azide **2** is most stable in its *S* = ½ state (D), as expected (Scheme S1). The *S* = 3/2 state (Q) was found to be 12.2. kcal/mol higher in energy. Through N_2 expulsion in **TS1** (+30.0 kcal/mol) intermediate **I-1** is formed. This intermediate also is most stable in the *S* = ½ state (0.7 kcal/mol). Insertion of the N into the Co-P bond through **TS2** results in intermediate **I-2**. The energies of the calculated spin states for **I-2** are very close with a difference of merely 0.7 kcal/mol and are therefore deemed equally stable. The conversion of **I-2** to **3** was not calculated. Different spin states of **3** were calculated (see Scheme S2): the energies of the quintet, heptet and triplet state are close to one another with a small preference for the latter. Calculations for the closed-shell singlet and open-shell singlet states of **3** did not converge.

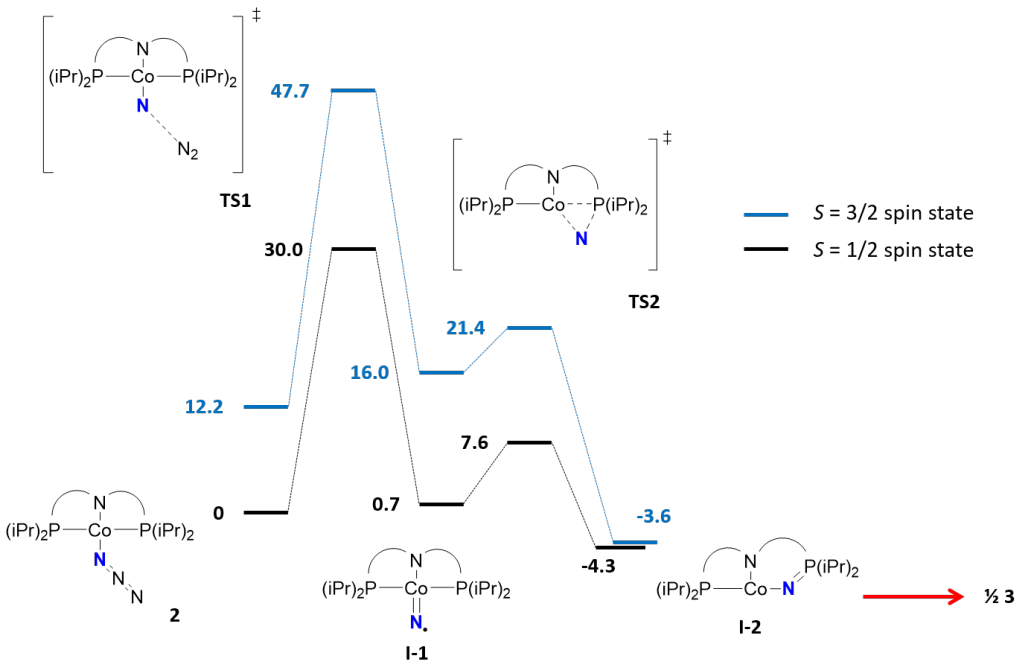

Scheme S1. DFT calculated free energy profile (ΔG^0_{298K} in kcal mol^{-1}) of the proposed pathway for formation of **3** upon photolysis/thermolysis of **2** (BP86-D3, def2-TZVP). Energies relative to *S* = ½ spin state of the starting material.

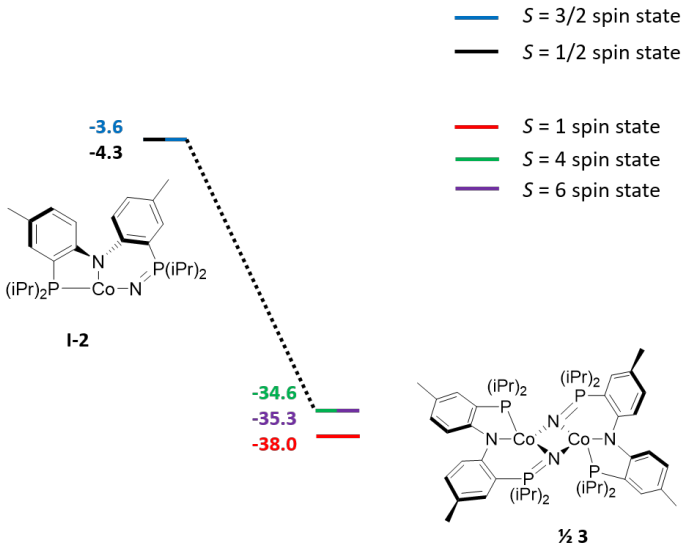

Scheme S2. Energies of different calculated spin states of **3** in kcal mol^{-1} relative to *S* = ½ spin state of starting material **2** (BP86-D3, def2-TZVP), the TS between **I-2** and **3** was not calculated but assumed to be accessible.

Table S1. Relative energies (kcal mol^{-1}) found for the optimized geometries (BP86-D3, def2-TZVP).

Structure	ΔG^0_{298K} in kcal mol^{-1}
2 (D)	0
2 (Q)	12.2
T1 (D)	30.0
T1 (Q)	47.7
I1 (D)	0.7
I1 (Q)	16.0
T2 (D)	7.6
T2 (Q)	21.4
I2 (D)	-4.3
I2 (Q)	-3.6
3 (*S* = 1)	-38.0
3 (*S* = 2)	-34.6
3 (*S* = 3)	-35.3

DFT calculations for Bond Order Analysis

	Wiberg BO	Mayer BO
Co-amido	0.518	0.528
Co -nitrido	1.777	1.949

Wiberg[S12] and Mayer[S13] bond orders were calculated from the Turbomole output files using the AOMix program.[S14]

6. Single Crystal X-ray Crystallography

Complex 4

X-ray intensities were measured on a Bruker D8 Quest Eco diffractometer equipped with a Triumph monochromator (λ = 0.71073 Å) and a CMOS Photon 50 detector at a temperature of 150(2) K. Intensity data were integrated with the Bruker APEX2 software.[S15] Absorption correction and scaling was performed with SADABS.[S16] The structures were solved using intrinsic phasing with the program SHELXT.[S15] Least-squares refinement was performed with SHELXL-2013[S17] against F^2 of all reflections. Non-hydrogen atoms were refined with anisotropic displacement parameters. The H atoms were placed at calculated positions using the instructions AFIX 13, AFIX 43 or AFIX 137 with isotropic displacement parameters having values 1.2 or 1.5 times *U*eq of the attached C atoms. CCDC for **4**: 1527630.

Complex 3

All reflection intensities were measured at 110(2) K using a SuperNova diffractometer (equipped with Atlas detector) with Cu *K*α radiation (λ = 1.54178 Å) under the program CrysAlisPro (Version 1.171.36.32 Agilent Technologies, 2013). The same program was used to refine the cell dimensions and for data reduction. The structure was solved with the program SHELXS-2014/7[S18] and was refined on F^2 with SHELXL-2014/7.[S18] Analytical numeric absorption correction using a multifaceted crystal model was applied using CrysAlisPro. The temperature of the data collection was controlled using the system Cryojet (manufactured by Oxford Instruments). The H atoms were placed at calculated positions using the instructions AFIX 13, AFIX 43 or AFIX 137 with isotropic displacement parameters having values 1.2 or 1.5 *U*eq of the attached C atoms. The structure is ordered. The asymmetric unit contains two crystallographically independent molecules (Z' = 2). CCDC for **3**: 1518623.

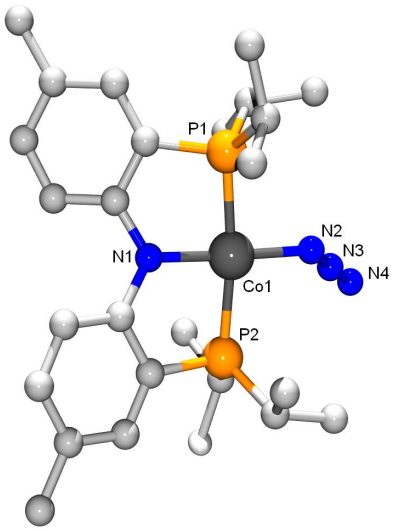

Figure S12. Preliminary connectivity plot for complex **2.**

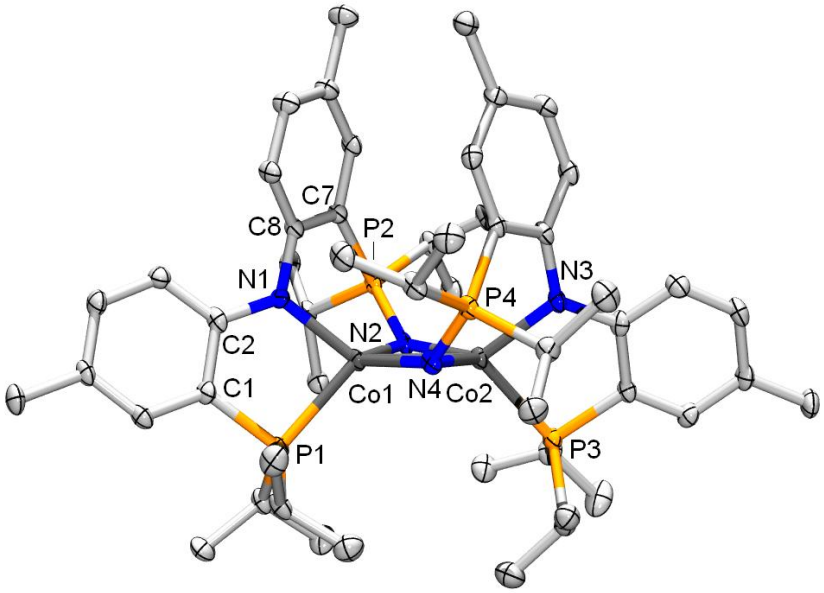

Figure S13. Displacement ellipsoid plot (50% probability level) of **3** at 110(2) K. Hydrogen atoms are omitted for clarity, selected bond lengths (Å) and angles (°): Co1-Co2 2.5679(8), Co1-N2 1.982(3), Co1-N4 1.927(3), Co2-N2 1.982(3), Co2-N4 1.989(3), Co1-P1 2.3148(11), Co2-P3 2.3313(11), P2-N2 1.580(3), Co1-N1 1.965(3), P4-N4 1.582(3), Co2-N3 1.976(3), Co1-N4-Co2 81.9(1), Co1-N2-Co2 81.8(1), N2-Co1-N4 97.97(12), N2-Co2-N4 97.39(12), C1-C2-C8-C7 65.4(7), C27-C28-C34-C33 63.1(7).

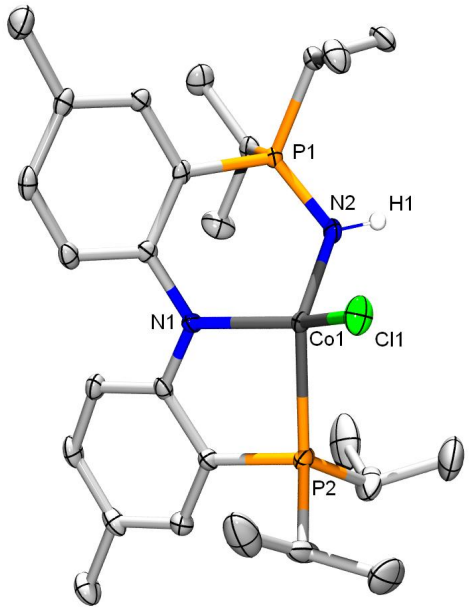

Figure S14. Displacement ellipsoid plot (50% probability level) of **4**. Hydrogen atoms omitted for clarity, except for H1 on N2. Selected bond lengths (Å) and angles (°): Co1-Cl1 2.2549(11); Co1-N1 1.959(3); Co1-N2 1.960(3); N2-P1 1.597(3); Co1-P2 2.3271(11); N1-Co1-P2 85.20(9); N2-Co1-P2 122.18(10); N1-Co1-Cl1 132.53(10); N1-Co1-N2 95.65(13); Co1-N2-P1 117.23(18).

7. References

S1 L. Fan, B. M. Foxman and O. V. Ozerov, *Organometallics*, 2004, **23**, 326–328.

S2 A. R. Fout, F. Basuli, H. Fan, J. Tomaszewski, J. C. Huffman, M. H. Baik and D. J. Mindiola, *Angew. Chem. Int. Ed.*, 2006, **45**, 3291–3295.

S3 The two bands may stem from multiple accessible conformations in solution: M. Käß, J. Hohenberger, M. Adelhardt, E. M. Zolnhofer, S. Mossin, F. W. Heinemann, J. Sutter and K. Meyer, *Inorg. Chem.*, 2014, **53**, 2460–2470.

S4 R. Ahlrichs, Turbomole version 6.5, Theoretical Chemistry Group, University of Karlsruhe.

S5 PQS version 2.4, 2001, Parallel Quantum Solutions, Fayettevile, Arkansas (USA); the Baker optimizer is available separately from PQS upon request: I. Baker, *J. Comput. Chem.*, 1986, **7**, 385–395.

S6 P. H. M. Budzelaar, *J. Comput. Chem.*, 2007, **28**, 2226–2236.

S7 A. D. Becke, *Phys. Rev. A*, 1988**, 38**, 3098–3100.

S8 J. P. Perdew, *Phys. Rev. B*, 1986, **33**, 8822-8824.

S9 F. Weigend and R. Ahlrichs, *Phys. Chem. Chem. Phys.*, 2005, **7**, 3297–3305.

S10 F. Weigend, M. Häser, H. Patzelt and R. Ahlrichs, *Chem. Phys. Lett.*, 1998, **294**, 143–152.

S11 S. Grimme, *J. Comput. Chem.*, 2006, **27**, 1787–1799.

S12 Wiberg, K. B. *Tetrahedron*, 1968, **24**, 1083.

S13 a) I. Mayer, *Chem. Phys. Lett.*, 1983, **97**, 270–274; b) I. Mayer, *Chem. Phys. Lett.*, 1984, **110**, 440–444; c) I. Mayer, *Int. J. Quantum Chem.*, 1986, **29**, 73–84; d) I. Mayer, *Int. J. Quantum Chem.*, 1986, **29**, 477–483; e) A. J. Bridgeman, G. Cavigliasso, L. R. Ireland and J. Rothery, *J. Chem. Soc., Dalton Trans.*, 2001, 2095–2108.

S14 a) S. I. Gorelsky, AOMix: Program for Molecular Orbital Analysis, http://www.sg-chem.net/, University of Ottawa, version 6.54, 2011; b) S. I. Gorelsky and A. B. P. Lever, *J. Organomet. Chem.*, 2001, **635**, 187–196.

S15 Bruker, *APEX2* software, Madison WI, USA, 2014.

S16 G. M. Sheldrick, *SADABS*, Universität Göttingen, Germany, 2008.

S17 G. M. Sheldrick, *SHELXL2013*, University of Göttingen, Germany, 2013.

S18 G. M. Sheldrick, *Acta Cryst.*, 2015, **C71**, 3-8